JACS
JOURNAL OF THE AMERICAN CHEMICAL SOCIETY
Cite This: J. Am. Chem. Soc. 2019, 141, 15761−15766
Communication
pubs.acs.org/JACS

Sequence-Defined Dendrons Dictate Supramolecular Cogwheel Assembly of Dendronized Perylene Bisimides

Benjamin E. Partridge,[†,□] Li Wang,[†,‡] Dipankar Sahoo,[†] James T. Olsen,[†] Pawaret Leowanawat,[†,○] Cecilé Roche,[†] Henrique Ferreira,[†] Kevin J. Reilly,[†] Xiangbing Zeng,[§] Goran Ungar,[§,⊥] Paul A. Heiney,[#] Robert Graf,[◊] Hans W. Spiess,[◊] and Virgil Percec*[,†]

[†]Roy & Diana Vagelos Laboratories, Department of Chemistry, University of Pennsylvania, Philadelphia, Pennsylvania 19104-6323, United States
[‡]College of Materials Science and Engineering, Beijing University of Chemical Technology, Beijing 100029, China
[§]Department of Materials Science and Engineering, University of Sheffield, Sheffield S1 3JD, United Kingdom
[⊥]State Key Laboratory for Mechanical Behavior of Materials, Xi'an Jiaotong University, Xi'an 710049, China
[#]Department of Physics and Astronomy, University of Pennsylvania, Philadelphia, Pennsylvania 19104-6396, United States
[◊]Max-Planck Institute for Polymer Research, 55128 Mainz, Germany

Supporting Information

ABSTRACT: A dendronized perylene bisimide (PBI) that self-organizes into hexagonal arrays of supramolecular double helices with identical single-crystal-like order that disregards chirality was recently reported. A cogwheel model of self-assembly that explains this process was proposed. Accessing the highly ordered cogwheel phase required very slow heating and cooling or extended periods of annealing. Analogous PBIs with linear alkyl chains did not exhibit the cogwheel assembly. Here a library of sequence-defined dendrons containing all possible compositions of linear and racemic alkyl chains was employed to construct self-assembling PBIs. Thermal and structural analysis of their assemblies by differential scanning calorimetry (DSC) and fiber X-ray diffraction (XRD) revealed that the incorporation of *n*-alkyl chains accelerates the formation of the high order cogwheel phase, rendering the previously invisible phase accessible under standard heating and cooling rates. Small changes to the primary structure, as constitutional isomerism, result in significant changes to macroscopic properties such as melting of the periodic array. This study demonstrated how changes to the sequence-defined primary structure, including the relocation of methyl groups between two constitutional isomers, dictate tertiary and quaternary structure in hierarchical assemblies. This led to the discovery of a sequence that self-organizes the cogwheel assembly much faster than even the corresponding homochiral compounds and demonstrated that defined-sequence, which has long been recognized as a determinant for the complex structure of biomacromolecules including proteins and nucleic acids, plays the same role also in supramolecular synthetic systems.

Function relies on hierarchical transfer of structural information from individual building blocks to supramolecular structure. Biomacromolecules such as proteins[1] and nucleic acids[2] require homochiral building blocks arranged in a defined-sequence with monodisperse chain length. In poly(propylene), the stereochemistry of methyl groups mediates function even with polydisperse chains.[3] This strategy to highly ordered structures and functions endows the demand for homochirality, defined-sequence, and monodisperse chains in biomacromolecules.[4]

Contrary to this expectation, a perylene bisimide (PBI) containing two chiral minidendrons (Figure 1a) was recently reported to form columnar hexagonal assemblies with single-crystal-like order irrespective of stereochemistry.[5] This contrasts examples[6−8] where the degree of order of 3D assemblies is determined by stereochemical purity. This enantiopure, racemic mixture of 21 diastereomeric dendronized PBIs self-organized into two distinct columnar hexagonal (Φ_h^k) crystalline arrays (Figure 1b): low order Φ_h^{k1} with PBI dimers stacked with 90° relative rotation and translated away from the column center and high order Φ_h^{k2} with dimers along the column axis, giving a smooth column exterior which enables ordered packing. Φ_h^{k2} was not observed at heating or cooling rates of 10 °C/min but required slow heating with 1 °C/min and was accidentally discovered by fiber XRD experiments while annealing the Φ_h^{k1} phase.

To rationalize this chirality-invariant crystallization of columns in Φ_h^{k2}, a *cogwheel model* that displays the alkyl chains of the PBI dendrons as "teeth" on a cogwheel was proposed.[5] These columns organize into single-handed homochiral crystal domains (Figure 1c), even for fully racemic samples such as **rrr-PBI** (Figure 1a). This cogwheel model has three key features (Figure 1d): (1) the length of the extended alkyl chains is equal to the helical half-pitch, ensuring the column periphery is covered in alkyl chains to maximize intercolumnar van der Waals interactions (Figure 1b); (2) the alkyl chains lie parallel to the column axis, limiting interdigitation of neighboring columns;

Received: August 16, 2019
Published: September 18, 2019

DOI: 10.1021/jacs.9b08714
J. Am. Chem. Soc. 2019, 141, 15761−15766

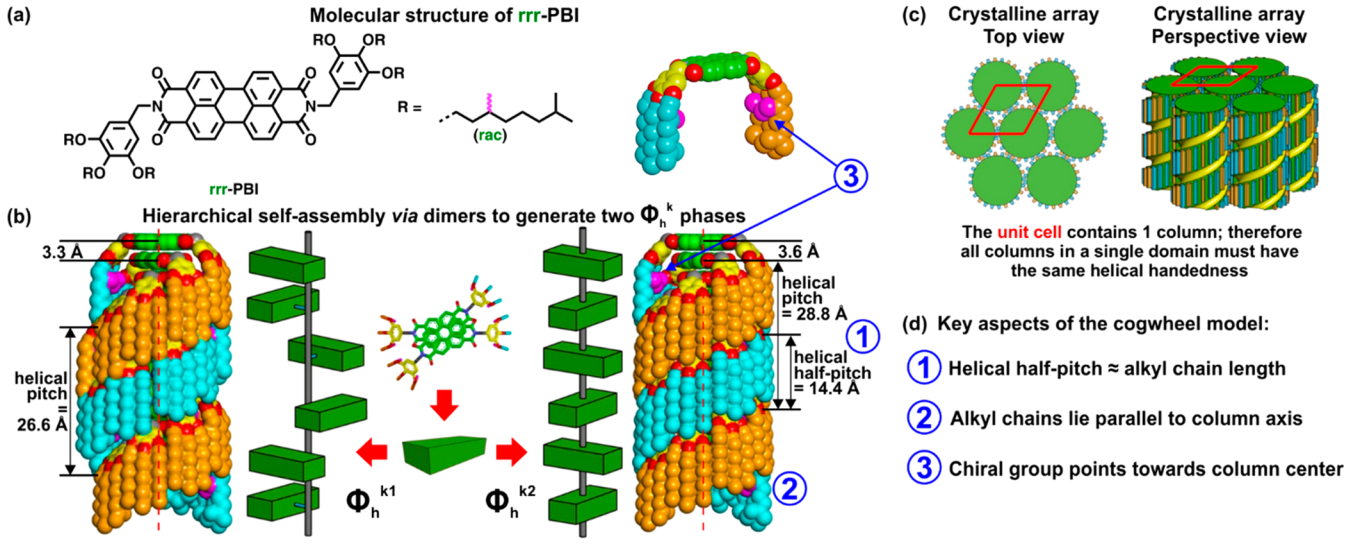

Figure 1. Cogwheel model of self-assembly.[7] (a) Molecular structure of **rrr-PBI**. The chiral methyl group is indicated in pink. (b) Two crystalline columnar hexagonal phases (Φ_h^{k1}, Φ_h^{k2}) are generated via hierarchical self-assembly of dimers rotated around the column axis. (c) The formation of a hexagonal crystalline array with only one helical column in the unit cell drives deracemization between columns. (d) Key aspects of the cogwheel model.

Scheme 1. Synthesis of PBIs with Sequence-Defined Linear Racemic Hybrid Minidendrons[a]

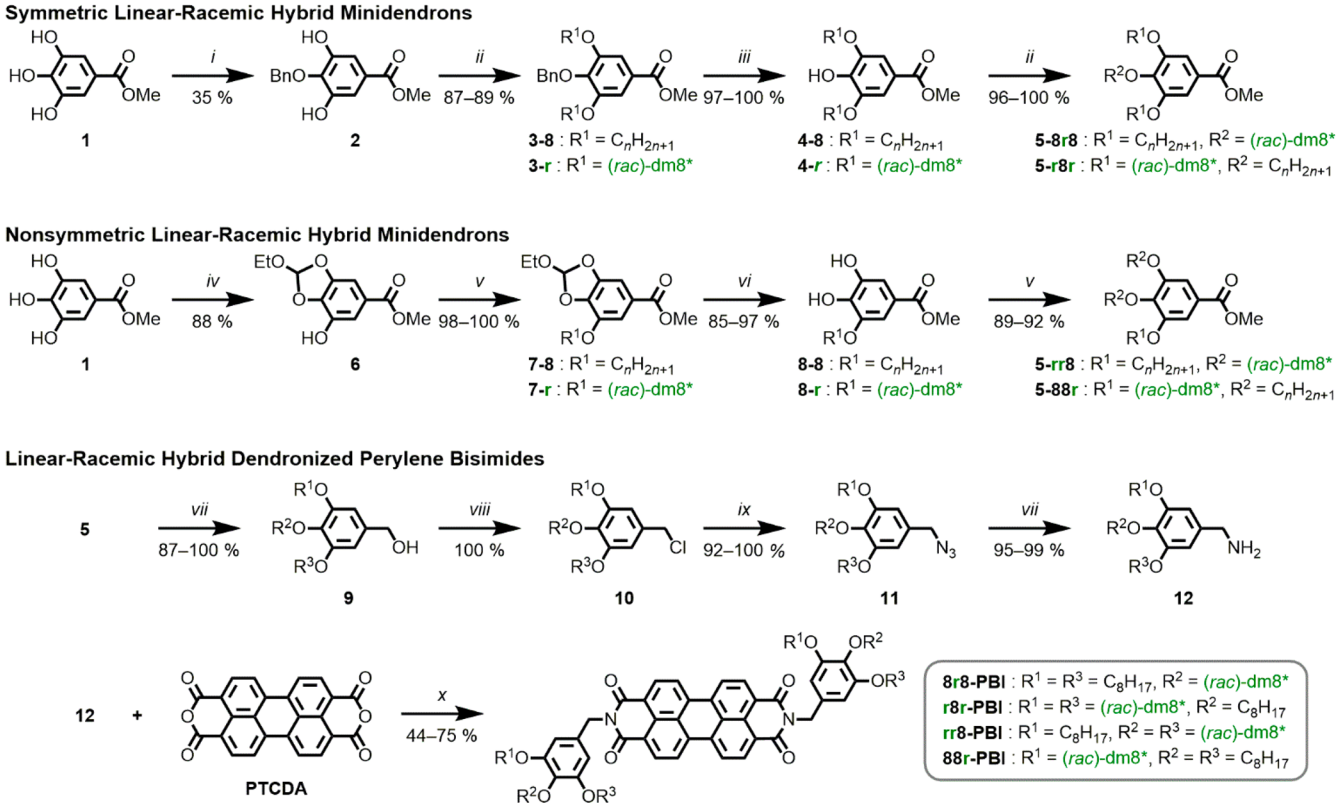

[a]Reagents and conditions: (*i*) BnCl, K_2CO_3, KI, acetone, reflux, 18 h; (*ii*) RBr, K_2CO_3, DMF, 120 °C, 3.5 h; (*iii*) H_2, Pd/C, CH_2Cl_2, MeOH, 23 °C, 24 h; (*iv*) triethyl orthoformate, Amberlyst-15(H), toluene, reflux, 18 h; (*v*) RBr, K_2CO_3, DMF, 65−70 °C, 4−7 h; (*vi*) 2 M HCl, methanol, 23 °C, 7 h; (*vii*) $LiAlH_4$, THF, 23 °C, 1 h; (*viii*) $SOCl_2$, *cat.* DMF, 23 °C, CH_2Cl_2, 0.5 h; (*ix*) NaN_3, DMF, 23 °C, 9 h; (*x*) PTCDA, $Zn(OAc)_2{\cdot}2H_2O$, quinoline, 180 °C, 6 h.

(3) the chiral methyl group on the dimethyloctyl (dm8*) chain points toward the column center, hiding the chirality of the stereocenter from the column periphery and thus eliminating its role in determining intercolumnar chiral interactions. This cogwheel model was not observed in PBI assemblies containing linear *n*-alkyl chains of any length.[9] This model (Figure 1)[5] does not predict the outcome of the replacement of dm8* with *n*-octyl to the self-organization of PBIs. This raises the simple question: how will PBIs with mixtures of linear and branched alkyl chains assemble? Answering this question is expected to

DOI: 10.1021/jacs.9b08714
J. Am. Chem. Soc. 2019, 141, 15761−15766

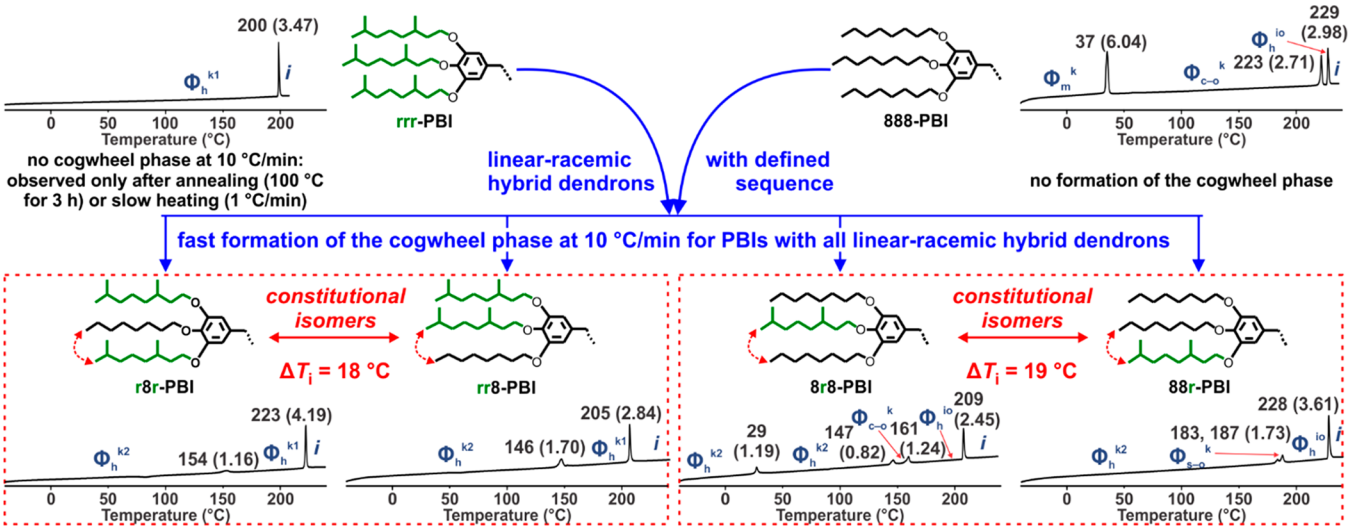

Figure 2. DSC traces of PBIs with hybrid dm8*/C8 dendrons measured upon heating the as-prepared sample at 10 °C/min. Phases determined by XRD, transition temperatures (in °C), and associated enthalpy changes (in parentheses, in kcal/mol) are indicated. Phase notation: Φ_h^{k1}—columnar hexagonal crystal with offset dimers.[5] Φ_h^{k2}—columnar hexagonal crystal with cogwheel assembly.[5] $\Phi_{c-o}{}^k$—columnar centered orthorhombic crystal. $\Phi_{s-o}{}^k$—columnar simple orthorhombic crystal. $\Phi_m{}^k$—columnar monoclinic crystal. Φ_h^{io}—2D columnar hexagonal phase with short-range intracolumnar order. *i*—isotropic.

provide valuable insights and to broaden the scope of the cogwheel model in self-assembly.

Sequence-defined structures[10] are fundamental to biomolecules[11] and have also been employed in self-assembling building blocks to assess protein−carbohydrate binding on biological cell membrane mimics.[12] Here, four dendronized PBIs with defined-sequences of *n*-octyl (also denoted **8** or C8) and branched dm8* chains (**r** or *rac*) on a (3,4,5)-minidendron were synthesized by iterative methodologies (Scheme 1). These compounds are identified by the placement of their chains in the 3-, 4-, and 5-positions: fully branched racemic **rrr-PBI**, fully linear **888-PBI**, symmetric hybrid **r8r-PBI** and **8r8-PBI**, and nonsymmetric hybrid **rr8-PBI** and **88r-PBI**. **r8r-PBI** is the constitutional isomer of **rr8-PBI** while **8r8-PBI** is that of **88r-PBI**.

Iterative methodologies were employed to construct the sequence of alkyl chains. Symmetric hybrid minidendrons were prepared from **2**, obtained via benzylation of methyl gallate (**1**).[13] Reaction of **1** with triethyl orthoformate gave nonsymmetric acetal-protected **6**,[14] which was employed for nonsymmetric dendrons. Alkylation of **2** and **6**, followed by deprotection, and additional alkylation provided sequence-defined dendrons **5**. ^{1}H and ^{13}C NMR, MALDI-TOF mass spectrometry, and HPLC confirmed the sequence-defined structure of dendrons **5** (Figures S1−S20). All benzyl esters **5** hybrid dendrons were subsequently converted to benzyl amines **12**. Imidation of perylene tetracarboxylic dianhydride (PTCDA) with **12** and $Zn(OAc)_2{\cdot}2H_2O$ in quinoline[9a] afforded **8r8-**, **r8r-**, **rr8-**, and **88r-PBI**.

The thermal behavior of the six dendronized PBIs, four sequence-defined hybrids plus **rrr-** and **888-PBI**, was measured by DSC with 10 °C/min (Figure 2, Figure S21). Phases were determined by fiber XRD. As already reported,[5] **rrr-PBI** assembles into a highly ordered 3D columnar hexagonal phase by the cogwheel model, denoted Φ_h^{k2}. This phase was not observed at 10 °C/min but required either heating with 1 °C/min or annealing at 100 °C for 3 h and cooling (Figure 2).[5] Only the columnar hexagonal phase, Φ_h^{k1}, was observed in the as-prepared sample upon heating and cooling **rrr-PBI** at 10 °C/min. The Φ_h^{k2} phase, formed by annealing, undergoes a transition to the Φ_h^{k1} phase at 128−130 °C upon heating (Figure S1).[5]

By contrast to **rrr-PBI**, which requires annealing to generate the Φ_h^{k2} phase, and to **888-PBI**, which does not self-organize into the Φ_h^{k2} phase (Figure 2, top), all four hybrid PBIs with dm8* and C8 chains self-organize into the cogwheel Φ_h^{k2} upon heating and cooling at 10 °C/min (Figure 2). This dramatic increase in rate of cogwheel assembly via the sequence-defined dendrons suggests that the linear chains dictate the formation of the Φ_h^{k2} phase, which is the thermodynamically favored but kinetically disfavored phase of **rrr-PBI** below 128−130 °C.

The Φ_h^{k2} of the four hybrid PBIs undergoes a transition upon heating. Hybrid PBIs with two dm8* chains (**r8r-** and **rr8-PBI**) form the Φ_h^{k1} phase at 152 and 146 °C, respectively, similar to **rrr-PBI**. By contrast, hybrid PBIs with two *n*-octyls (**8r8-** and **88r-PBI**) generate orthorhombic and 2D hexagonal phases upon heating, similar to **888-PBI**. Therefore, the majority chain dictates the supramolecular structure generated by the hybrid PBIs: dendrons with more dm8* chains, **r8r-**, **rr8-PBI**, self-organize identical phases as **rrr-PBI** and are sequences of interest for physical investigations, whereas dendrons with more *n*-octyls self-organize into similar phases to **888-PBI**. Upon cooling all four hybrids reform Φ_h^{k2}.

The isotropization temperatures (T_i) of the hybrid PBIs depend on the number of linear chains and the nature of the chain in the 4-position of the dendron. Dendrons with 4-dm8* exhibit T_i values similar to **rrr-PBI** (T_i of **rrr-**, **rr8-**, and **8r8-PBI** = 200, 205, 209 °C) whereas those with an *n*-octyl in the 4-position exhibit T_i values more similar to **888-PBI** (T_i of **r8r-**, **88r-**, and **888-PBI** = 223, 228, 229 °C). It is notable that T_i, which is indicative of quaternary structure, differs by almost 20 °C between constitutionally isomeric hybrid PBIs (red boxes in Figure 2) and spans 30 °C across this entire set of very similar primary structures.

Oriented fiber XRD was used to elucidate the structures of hybrid PBI assemblies.[15] Fiber XRD patterns of **rrr-PBI** (Figure S22a) and the four hybrid PBIs (Figure S22b−e) are consistent with the cogwheel Φ_h^{k2} phase (Table ST2). Lattice parameters of the Φ_h^{k2} unit cell of these five PBIs are identical, $a = 26.7 \pm 0.4$

DOI: 10.1021/jacs.9b08714
J. Am. Chem. Soc. 2019, 141, 15761−15766

Å and $c = 14.8 \pm 0.1$ Å. Experimental densities of the PBIs range from 1.05 g/cm^3 to 1.07 g/cm^3 (Table ST3), and the calculated number of molecules per column stratum, μ, is 0.97−1.08, that is, 1 molecule. The distance between strata, which corresponds to the average $\pi-\pi$ stacking distance, is 3.7 ± 0.05 Å, and the column diameter ($D_{col} = a$) is 26.7 ± 0.4 Å. The phases of **888-PBI** have been reported.[9c] At 80 °C, **888-PBI** exhibits a Φ_{c-o}^{k} phase with D_{col} = 24.2 Å, μ = 1.01, and a $\pi-\pi$ distance of 3.6 Å (Figure S22f).

XRD demonstrates the enhanced rate of formation of the cogwheel Φ_h^{k2} in hybrid PBIs compared to **rrr-PBI** (Figure 3).

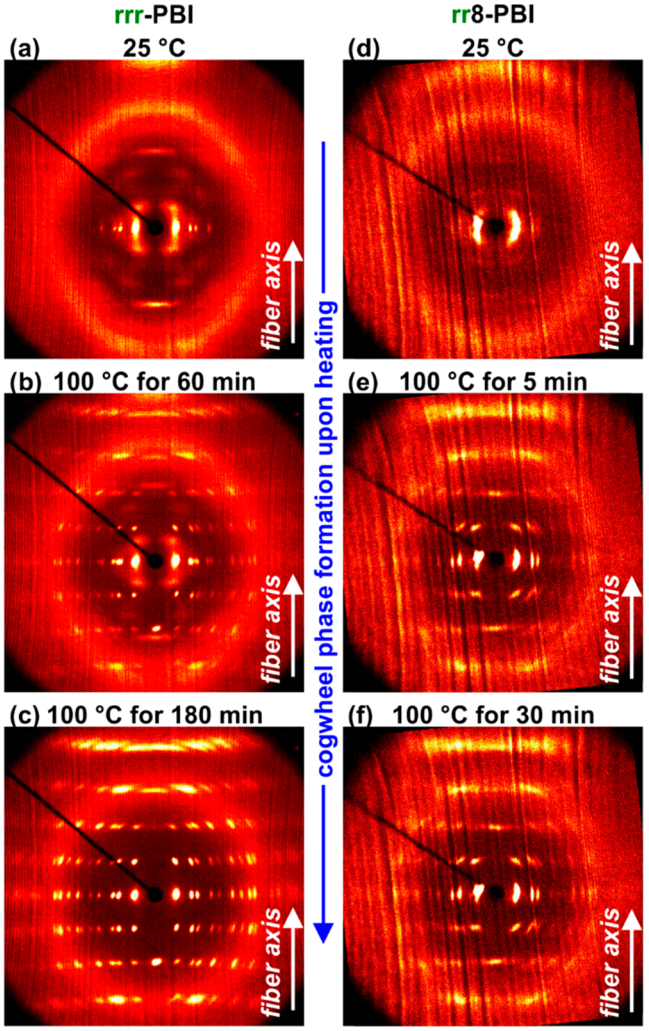

Figure 3. Formation of Φ_h^{k2} upon heating. (a−c) XRD patterns of **rrr-PBI** recorded at (a) 25 °C after 5 min and (b, c) 100 °C after (b) 60 and (c) 180 min. (d−f) XRD patterns of **rr8-PBI** recorded at (d) 25 °C after 5 min and (e, f) 100 °C after (e) 5 and (f) 30 min. Fiber axis indicated. Data collection time for each pattern was 5 min, and hence, data collection of e started as soon as the sample reached 100 °C.

Heating the Φ_h^{k1} of **rrr-PBI** to 100 °C at 10 °C/min does not generate high order Φ_h^{k2}. After annealing at 100 °C for 60 min, coexistence of the Φ_h^{k1} and Φ_h^{k2} is observed by XRD (Figure 3b). Continued annealing at 100 °C provides only the Φ_h^{k2} after 3 h (Figure 3c). In contrast, heating the hybrid PBIs generates Φ_h^{k2} immediately at 100 °C, as shown for **rr8-PBI** in Figure 3e. Further annealing at 100 °C does not change the XRD pattern (Figure 3f), supporting that the ordered Φ_h^{k2} is fully generated within minutes (Figure 3e). This dramatic enhancement of the rate of formation of the Φ_h^{k2} in hybrid PBIs could not be predicted and suggests that the linear alkyl chains dictate ordering of the branched dm8* chains to generate the cogwheel system. This thermal behavior (Figure 2) suggests that the Φ_h^{k2} of **rrr-PBI** and the four hybrid PBIs cannot be strictly identical, contrary to the highly similar lattice parameters determined by XRD (Figure S22 and Table ST2).

Solid state NMR reveals information about dynamics on a time scale much longer than XRD.[16] ^{13}C cross-polarization magic angle spinning NMR experiments of the hybrid PBIs (Figure S23) show only subtle differences for signals corresponding to C═O, the dendron phenyl ring, and −NCH_2−, suggesting that the packing of the dendron and stacking of the PBI core are almost identical, consistent with XRD data. Hence differences between the supramolecular packing of the four hybrid PBIs are driven mostly by the conformations of the *n*-alkyl chains. NMR suggests that *n*-alkyls in *m*- and *p*-positions increase local mobility at the stereogenic center, providing faster crystallization (Figure S23). Therefore, disorder creates order.[4a,b] Modeling of similar supramolecular assemblies does not typically consider the structure of the aliphatic region.[9,17] Demonstration of a hat-shaped cyclotriveratrylene that undergoes supramolecular deracemization provides a rare example of the *n*-alkyl conformation being elucidated.[6c] A detailed cogwheel model that accounts for *n*-alkyl conformation is under investigation.

The cogwheel model enables the generation of identical, highly ordered helical hexagonal crystals that disregard chirality. This work demonstrated that incorporation of *n*-alkyls into dendronized PBIs with chiral racemic chains transforms the invisible cogwheel Φ_h^{k2} into a kinetically accessible, visible phase, via a sequence-defined dendron. The composition and the sequence of the dendrons in hybrid linear-racemic PBIs dictates significant differences in their thermal behavior, even between constitutional isomers. This demonstrates that very minor sequence changes to the primary structure of a building block dictate substantial changes to macroscopic functions.

■ ASSOCIATED CONTENT

Supporting Information

The Supporting Information is available free of charge on the ACS Publications website at DOI: 10.1021/jacs.9b08714.

Synthetic procedures with complete characterization data, experimental methods, structural and thermal analysis parameters, and additional discussion (PDF)

■ AUTHOR INFORMATION

Corresponding Author

*percec@sas.upenn.edu

ORCID

Benjamin E. Partridge: 0000-0003-2359-1280
Goran Ungar: 0000-0002-9743-2656
Hans W. Spiess: 0000-0002-4779-654X
Virgil Percec: 0000-0001-5926-0489

Present Addresses

□B.E.P.: Department of Chemistry and International Institute of Nanotechnology, Northwestern University, Evanston, Illinois 60208, United States.

DOI: 10.1021/jacs.9b08714
J. Am. Chem. Soc. 2019, 141, 15761−15766

[○]P.L.: Department of Chemistry and Center of Excellence for Innovation in Chemistry, Mahidol University, Bangkok 10400, Thailand.

Notes

The authors declare no competing financial interest.

■ ACKNOWLEDGMENTS

Financial support by the National Science Foundation (DMR-1066116 and DMR-1807127 (V.P.), DMR-1120901 (V.P. and P.A.H.)), the Humboldt Foundation (V.P.), and the P. Roy Vagelos Chair at Penn (V.P.) is gratefully acknowledged. B.E.P. thanks the Howard Hughes Medical Institute for an International Student Research Fellowship.

■ REFERENCES

(1) Nanda, V.; Andrianarijaona, A.; Narayanan, C. The Role of Protein Homochirality in Shaping the Energy Landscape of Folding. *Protein Sci.* **2007**, *16*, 1667−1675.

(2) (a) Chen, Z.; Lichtor, P. C.; Berliner, A. P.; Chen, J. C.; Liu, D. R. Evolution of Sequence-Defined Highly Functionalized Nucleic Acid Polymers. *Nat. Chem.* **2018**, *10*, 420−427. (b) Cecconello, A.; Simmel, F. C. Controlling Chirality across Length Scales Using DNA. *Small* **2019**, *15*, 1805419.

(3) Natta, G.; Pino, P.; Corradini, P.; Danusso, F.; Moraglio, G.; Mantica, E.; Mazzanti, G. Crystalline High Polymers of α-Olefins. *J. Am. Chem. Soc.* **1955**, *77*, 1708−1710.

(4) (a) Kauffman, S. A.; *The Origins of Order: Self-Organization and Selection in Evolution*; Oxford University Press: New York, 1993. (b) Kauffman, S.; *At Home in the Universe: The Search for the Laws of Self-Organization and Complexity*; Oxford University Press: New York, 1995. (c) Fujii, N.; Saito, T. Homochirality and Life. *Chem. Rec.* **2004**, *4*, 267−278. (d) Blackmond, D. G. The Origin of Biological Homochirality. *Cold Spring Harbor Perspect. Biol.* **2010**, *2*, a002147. (e) Percec, V.; Leowanawat, P. Why Are Biological Systems Homochiral? *Isr. J. Chem.* **2011**, *51*, 1107−1117.

(5) Roche, C.; Sun, H.-J.; Leowanawat, P.; Araoka, F.; Partridge, B. E.; Peterca, M.; Wilson, D. A.; Prendergast, M. E.; Heiney, P. A.; Graf, R.; Spiess, H. W.; Zeng, X.; Ungar, G.; Percec, V. A Supramolecular Helix That Disregards Chirality. *Nat. Chem.* **2016**, *8*, 80−89.

(6) (a) Percec, V.; Dulcey, A. E.; Balagurusamy, V. S. K.; Miura, Y.; Smidrkal, J.; Peterca, M.; Nummelin, S.; Edlund, U.; Hudson, S. D.; Heiney, P. A.; Duan, H.; Magonov, S. N.; Vinogradov, S. A. Self-Assembly of Amphiphilic Dendritic Dipeptides into Helical Pores. *Nature* **2004**, *430*, 764−768. (b) Rosen, B. M.; Peterca, M.; Morimitsu, K.; Dulcey, A. E.; Leowanawat, P.; Resmerita, A.-M.; Imam, M. R.; Percec, V. Programming the Supramolecular Helical Polymerization of Dendritic Dipeptides *via* the Stereochemical Information of the Dipeptide. *J. Am. Chem. Soc.* **2011**, *133*, 5135−5151. (c) Roche, C.; Sun, H.-J.; Prendergast, M. E.; Leowanawat, P.; Partridge, B. E.; Heiney, P. A.; Araoka, F.; Graf, R.; Spiess, H. W.; Zeng, X.; Ungar, G.; Percec, V. Homochiral Columns Constructed by Chiral Self-Sorting During Supramolecular Helical Organization of Hat-Shaped Molecules. *J. Am. Chem. Soc.* **2014**, *136*, 7169−7185.

(7) (a) Markvoort, A. J.; ten Eikelder, H. M. M.; Hilbers, P. A. J.; de Greef, T. F. A.; Meijer, E. W. Theoretical Models of Nonlinear Effects in Two-Component Cooperative Supramolecular Copolymerizations. *Nat. Commun.* **2011**, *2*, 509. (b) Helmich, F.; Smulders, M. M. J.; Lee, C. C.; Schenning, A. P. H. J.; Meijer, E. W. Effect of Stereogenic Centers on the Self-Sorting, Depolymerization, and Atropisomerization Kinetics of Porphyrin-Based Aggregates. *J. Am. Chem. Soc.* **2011**, *133*, 12238−12246. (c) Kulkarni, C.; Berrocal, J. A.; Lutz, M.; Palmans, A. R. A.; Meijer, E. W. Directing the Solid-State Organization of Racemates via Structural Mutation and Solution-State Assembly Processes. *J. Am. Chem. Soc.* **2019**, *141*, 6302−6309. (d) Yashima, E.; Ousaka, N.; Taura, D.; Shimomura, K.; Ikai, T.; Maeda, K. Supramolecular Helical Systems: Helical Assemblies of Small Molecules, Foldamers, and Polymers with Chiral Amplification and Their Functions. *Chem. Rev.* **2016**, *116*, 13752−13990. (e) Hill, D. J.; Mio, M. J.; Prince, R. B.; Hughes, T. S.; Moore, J. S. A Field Guide to Foldamers. *Chem. Rev.* **2001**, *101*, 3893−4012.

(8) (a) Venkata Rao, K.; Miyajima, D.; Nihonyanagi, A.; Aida, T. Thermally Bisignate Supramolecular Polymerization. *Nat. Chem.* **2017**, *9*, 1133−1139. (b) Yano, K.; Itoh, Y.; Araoka, F.; Watanabe, G.; Hikima, T.; Aida, T. Nematic-to-Columnar Mesophase Transition by *in situ* Supramolecular Polymerization. *Science* **2019**, *363*, 161−165. (c) Krieg, E.; Bastings, M. M. C.; Besenius, P.; Rybtchinski, B. Supramolecular Polymers in Aqueous Media. *Chem. Rev.* **2016**, *116*, 2414−2477. (d) Freire, F.; Quiñoá, E.; Riguera, R. Supramolecular Assemblies from Poly(phenylacetylene)s. *Chem. Rev.* **2016**, *116*, 1242−1271. (e) Cobos, K.; Quiñoá, E.; Riguera, R.; Freire, F. Chiral-to-Chiral Communication in Polymers: A Unique Approach To Control Both Helical Sense and Chirality at the Periphery. *J. Am. Chem. Soc.* **2018**, *140*, 12239−12246.

(9) (a) Percec, V.; Peterca, M.; Tadjiev, T.; Zeng, X.; Ungar, G.; Leowanawat, P.; Aqad, E.; Imam, M. R.; Rosen, B. M.; Akbey, U.; Graf, R.; Sekharan, S.; Sebastiani, D.; Spiess, H. W.; Heiney, P. A.; Hudson, S. D. Self-Assembly of Dendronized Perylene Bisimides into Complex Helical Columns. *J. Am. Chem. Soc.* **2011**, *133*, 12197−12219. (b) Percec, V.; Hudson, S. D.; Peterca, M.; Leowanawat, P.; Aqad, E.; Graf, R.; Spiess, H. W.; Zeng, X.; Ungar, G.; Heiney, P. A. Self-Repairing Complex Helical Columns Generated *via* Kinetically Controlled Self-Assembly of Dendronized Perylene Bisimides. *J. Am. Chem. Soc.* **2011**, *133*, 18479−18494. (c) Percec, V.; Sun, H.-J.; Leowanawat, P.; Peterca, M.; Graf, R.; Spiess, H. W.; Zeng, X.; Ungar, G.; Heiney, P. A. Transformation from Kinetically into Thermodynamically Controlled Self-Organization of Complex Helical Columns with 3D Periodicity Assembled from Dendronized Perylene Bisimides. *J. Am. Chem. Soc.* **2013**, *135*, 4129−4148.

(10) (a) Tomalia, D. A.; Naylor, A. M.; Goddard, W. A. Starburst Dendrimers: Molecular-Level Control of Size, Shape, Surface Chemistry, Topology and Flexibility from Atom to Macroscopic Matter. *Angew. Chem., Int. Ed. Engl.* **1990**, *29*, 138−175. (b) Hawker, C. J.; Frechet, J. M. J. Preparation of Polymers with Controlled Molecular Architecture. A New Convergent Approach to Dendritic Macromolecules. *J. Am. Chem. Soc.* **1990**, *112*, 7638−7647. (c) Leibfarth, F. A.; Johnson, J. A.; Jamison, T. F. Scalable Synthesis of Sequence-Defined Unimolecular Macromolecules by Flow-IEG. *Proc. Natl. Acad. Sci. U. S. A.* **2015**, *112*, 10617−10622. (d) Xu, J.; Fu, C.; Shanmugam, S.; Hawker, C. J.; Moad, G.; Boyer, C. Synthesis of Discrete Oligomers by Sequential PET-RAFT Single-Unit Monomer Insertion. *Angew. Chem., Int. Ed.* **2017**, *56*, 8376−8383. (e) Dong, R.; Liu, R.; Gaffney, P. R. J.; Schaepertoens, M.; Marchetti, P.; Williams, C. R.; Chen, R.; Livingston, A. G. Sequence-Defined Multifunctional Polyethers *via* Liquid-Phase Synthesis with Molecular Sieving. *Nat. Chem.* **2019**, *11*, 136−145. (f) Yue, K.; Huang, M.; Marson, R. L.; He, J.; Huang, J.; Zhou, Z.; Wang, J.; Liu, C.; Yan, X.; Wu, K.; Guo, Z.; Liu, H.; Zhang, W.; Ni, P.; Wesdemiotis, C.; Zhang, W.-B.; Glotzer, S. C.; Cheng, S. Z. D. Geometry Induced Sequence of Nanoscale Frank−Kasper and Quasicrystal Mesophases in Giant Surfactants. *Proc. Natl. Acad. Sci. U. S. A.* **2016**, *113*, 14195−14200. (g) Zhang, W.; Lu, X.; Mao, J.; Hsu, C.-H.; Mu, G.; Huang, M.; Guo, Q.; Liu, H.; Wesdemiotis, C.; Li, T.; Zhang, W.-B.; Li, Y.; Cheng, S. Z. D. Sequence-Mandated, Distinct Assembly of Giant Molecules. *Angew. Chem., Int. Ed.* **2017**, *56*, 15014−15019.

(11) (a) Zuckermann, R. N.; Kerr, J. M.; Kent, S. B. H.; Moos, W. H. Efficient Method for the Preparation of Peptoids [Oligo(*N*-substituted Glycines]) by Submonomer Solid-Phase Synthesis. *J. Am. Chem. Soc.* **1992**, *114*, 10646−10647. (b) Caruthers, M. H. Gene Synthesis Machines: DNA Chemistry and Its Uses. *Science* **1985**, *230*, 281−285. (c) Caruthers, M. H. The Chemical Synthesis of DNA/RNA: Our Gift to Science. *J. Biol. Chem.* **2013**, *288*, 1420−1427. (d) Plante, O. J.; Palmacci, E. R.; Seeberger, P. H. Automated Solid-Phase Synthesis of Oligosaccharides. *Science* **2001**, *291*, 1523−1527. (e) Guberman, M.; Seeberger, P. H. Automated Glycan Assembly: A Perspective. *J. Am. Chem. Soc.* **2019**, *141*, 5581−5592.

DOI: 10.1021/jacs.9b08714
J. Am. Chem. Soc. 2019, 141, 15761−15766

(12) (a) Zhang, S.; Xiao, Q.; Sherman, S. E.; Muncan, A.; Ramos Vicente, A. D. M.; Wang, Z.; Hammer, D. A.; Williams, D.; Chen, Y.; Pochan, D. J.; Vértesy, S.; André, S.; Klein, M. L.; Gabius, H.-J.; Percec, V. Glycodendrimersomes from Sequence-Defined Janus Glycodendrimers Reveal High Activity and Sensor Capacity for the Agglutination by Natural Variants of Human Lectins. *J. Am. Chem. Soc.* **2015**, *137*, 13334−13344. (b) Xiao, Q.; Zhang, S.; Wang, Z.; Sherman, S. E.; Moussodia, R.-O.; Peterca, M.; Muncan, A.; Williams, D. R.; Hammer, D. A.; Vértesy, S.; André, S.; Gabius, H.-J.; Klein, M. L.; Percec, V. Onion-like Glycodendrimersomes from Sequence-Defined Janus Glycodendrimers and Influence of Architecture on Reactivity to a Lectin. *Proc. Natl. Acad. Sci. U. S. A.* **2016**, *113*, 1162−1167. (c) Kopitz, J.; Xiao, Q.; Ludwig, A.-K.; Romero, A.; Michalak, M.; Sherman, S. E.; Zhou, X.; Dazen, C.; Vertésy, S.; Kaltner, H.; Klein, M. L.; Gabius, H.-J.; Percec, V. Reaction of a Programmable Glycan Presentation of Glycodendrimersomes and Cells with Engineered Human Lectins to Show the Sugar Functionality of the Cell Surface. *Angew. Chem., Int. Ed.* **2017**, *56*, 14677−14681. (d) Xiao, Q.; Ludwig, A.-K.; Romano, C.; Buzzacchera, I.; Sherman, S. E.; Vetro, M.; Vertésy, S.; Kaltner, H.; Reed, E. H.; Möller, M.; Wilson, C. J.; Hammer, D. A.; Oscarson, S.; Klein, M. L.; Gabius, H.-J.; Percec, V. Exploring Functional Pairing Between Surface Glycoconjugates and Human Galectins Using Programmable Glycodendrimersomes. *Proc. Natl. Acad. Sci. U. S. A.* **2018**, *115*, E2509−E2518. (e) Rodriguez-Emmenegger, C.; Xiao, Q.; Kostina, N. Y.; Sherman, S. E.; Rahimi, K.; Partridge, B. E.; Li, S.; Sahoo, D.; Reveron Perez, A. M.; Buzzacchera, I.; Han, H.; Kerzner, M.; Malhotra, I.; Möller, M.; Wilson, C. J.; Good, M. C.; Goulian, M.; Baumgart, T.; Klein, M. L.; Percec, V. Encoding Biological Recognition in a Bicomponent Cell-Membrane Mimic. *Proc. Natl. Acad. Sci. U. S. A.* **2019**, *116*, 5376−5382.

(13) Pearson, A. J.; Bruhn, P. R. Studies on the Synthesis of Aryl Ethers Using Arene-Manganese Chemistry. *J. Org. Chem.* **1991**, *56*, 7092−7097.

(14) Percec, V.; Imam, M. R.; Peterca, M.; Wilson, D. A.; Heiney, P. A. Self-Assembly of Dendritic Crowns into Chiral Supramolecular Spheres. *J. Am. Chem. Soc.* **2009**, *131*, 1294−1304.

(15) Peterca, M.; Percec, V.; Imam, M. R.; Leowanawat, P.; Morimitsu, K.; Heiney, P. A. Molecular Structure of Helical Supramolecular Dendrimers. *J. Am. Chem. Soc.* **2008**, *130*, 14840−14852.

(16) (a) Hansen, M. R.; Graf, R.; Spiess, H. W. Solid-State NMR in Macromolecular Systems: Insights on How Molecular Entities Move. *Acc. Chem. Res.* **2013**, *46*, 1996−2007. (b) Hansen, M. R.; Graf, R.; Spiess, H. W. Interplay of Structure and Dynamics in Functional Macromolecular and Supramolecular Systems as Revealed by Magnetic Resonance Spectroscopy. *Chem. Rev.* **2016**, *116*, 1272−1308.

(17) Herbst, S.; Soberats, B.; Leowanawat, P.; Lehmann, M.; Würthner, F. A Columnar Liquid-Crystal Phase Formed by Hydrogen-Bonded Perylene Bisimide J-Aggregates. *Angew. Chem., Int. Ed.* **2017**, *56*, 2162−2165.

DOI: 10.1021/jacs.9b08714
J. Am. Chem. Soc. 2019, 141, 15761−15766